



Supplementary Information for

Efficient CRISPR-mediated base editing in *Agrobacterium* spp.

Savio D. Rodrigues, Mansour Karimi, Lennert Impens, Els Van Lerberge, Griet Coussens, Stijn Aesaert, Debbie Rombaut, Dominique Holtappels, Heba M.M. Ibrahim, Marc Van Montagu*, Jeroen Wagemans, Thomas B. Jacobs, Barbara De Coninck* and Laurens Pauwels*

E-mail: marc.vanmontagu@ugent.be; barbara.deconinck@kuleuven.be;
laurens.pauwels@psb.vib-ugent.be

This PDF file includes:

SI Materials and Methods
Figures S1 to S9
Tables S1 to S3
Legends for Datasets S1 to S3
SI References

Other supplementary materials for this manuscript include the following:

Datasets S1 to S3

SI MATERIALS AND METHODS

Strains, media, and conditions. *E. coli* DH5 α competent cells (Thermo Fisher Scientific) and *ccdB* survival cells (Invitrogen) were used as cloning hosts. The Luria Bertani (LB) medium (5 g/L yeast extract, 10 g/L tryptone, 10 g/L NaCl, and 15 g/L agar) was used as the routine growth medium with following antibiotic concentrations: 100 μ g/mL spectinomycin, 25 μ g/mL chloramphenicol, and 50 μ g/mL kanamycin. Strains were grown at 37°C.

A. tumefaciens strains EHA101 (1) and EHA105 (2) were grown on yeast extract beef (YEB) medium (1 g/L yeast extract, 5 g/L peptone, 5 g/L sucrose, 5 g/L beef extract, 2 mM MgSO₄, and 15 g/L agar) supplemented with following antibiotic concentrations: 100 μ g/mL spectinomycin and 100 μ g/mL rifampicin. When *sacB* was used, the LB medium was utilized for selection after transformation and sucrose-supplemented (10%; wt/vol) YEB for curing, unless stated otherwise. *A. rhizogenes* strain K599 (National Council for Plant Pathogenic Bacteria Central Science Laboratory, <http://www.ncppb.com>) was grown on yeast extract peptone (YEP) medium (10 g/L yeast extract, 10 g/L peptone, 5 g/L NaCl, and 15 g/L agar) supplemented with the appropriate antibiotics, except in the case of *sacB*, for which AT minimal medium (3) was used supplemented with glucose (0.5%; wt/vol) or with sucrose (10%; wt/vol) with the appropriate antibiotics, 300 μ g/mL streptomycin and 100 μ g/mL spectinomycin for selection after transformation and for curing alone (4). All *Agrobacterium* strains were grown at 28°C. All bacterial strains used are detailed in *SI Appendix*, Table S1.

CRISPR/Cas9 vector construction.

Promoter cloning - The constitutive promoter driving the *aadA* gene was cloned with the primers AgroPromo1F and AgroPromo1R (*SI Appendix*, Table S2) and pZP200 (5) as a template. After purification, the polymerase chain reaction (PCR) product was cut with BsaI and the fragments were ligated into the BsaI site of the pGGA000 (6) to generate pGG-A-PAGROI-B.

Terminator cloning - Primers D_Stop_T3Ter_GF 56 and D_Stop_T3Ter_GR 56 (*SI Appendix*, Table S2) were used generate a double-stranded T3 terminator (7) with a stop codon that was cloned into the pGGD-G vector to yield pGG-D-T3T-G.

SpCas9 cloning - The *SpCas9*-coding sequence was amplified from JX560337 (pSEVA421-Cas9-tracrRNA) (8) with the primers SEVA421Cas9F/R (*SI Appendix*, Table S2) and cloned into pGGC000 (6) via Gibson assembly to generate pGG-C-SpCas9-D. A correct clone was verified by Sanger sequencing of the entire coding sequence. pGG-C-SpCas9-D was then assembled into pEN-L4-AG-R1 (9) with pGG-A-PAGROI-B, pGG-B-Linker-C, and pGG-D-T3T-G to generate pEN-L4-PAGROI-SpCas9-T3T-R1. A correct clone was verified by a restriction digest with PvuII and NheI.

sgRNA module - Two long primers J23119B1B1ScF (ACCT-PJ23119-BsaI-BsaI-Scaf forward) and J23119B1B1ScR2 (ATAC-PJ23119-BsaI-BsaI-Scaf reverse) (Scaf, sgRNA scaffold; *SI Appendix*, Table S2) were hybridized to make double-stranded oligonucleotides. The

pEN-L1-AG-L2 vector (9) was digested with BsaI and the vector fragment was purified from gel. The linearized pEN-L1-AG-L2 was ligated to the double-stranded oligonucleotide to generate pEN-L1-PJ23119-BsaI-BsaI-Scaf-L2. To reduce false-positive background, a *ccdB*-CmR cassette was amplified from pPGW (<https://gatewayvectors.vib.be>) with the primers *ccdBAgroF* and *ccdBAgroR* (*SI Appendix*, Table S2); then the PCR product was purified and digested by BsaI, thereafter the digest was purified. pEN-L1-PJ23119-BsaI-BsaI-Scaf-L2 was linearized by BsaI and was ligated to the *ccdB*-CmR fragment to generate pEN-L1-PJ23119-BsaI-*ccdB*-CmR-BsaI-Scaf-L2. For selection based on the green fluorescent protein (GFP) expression, BsaI-*PglpT*-sfGFP-*TrrfB*-BsaI (10) was added for easy cloning of the spacers and yielded pEN-L1-PJ23119-BsaI-*PglpT*-sfGFP-*TrrfB*-BsaI-Scaf-L2.

sgRNA cloning - Appropriate 18- to 22-bp spacers were ordered as complementary oligonucleotides (Integrated DNA Technologies, Leuven, Belgium) (*SI Appendix*, Table S2) with BsaI-compatible ends. Oligonucleotides were annealed to obtain the desired double-stranded spacer components. The assembled spacers and the pEN-L1-PJ23119-BsaI-*ccdB*-CmR-BsaI-Scaf-L2 or pEN-L1-J23119-BsaI-*PglpT*-sfGFP-*TrrfB*-BsaI-Scaf-L2 vectors were subjected to restriction digest with BsaI-HF (New England Biolabs). The restriction digest products were ligated with T4-DNA ligase (New England Biolabs) and transformed to *E. coli*. In case of the GFP dropout construct, white colonies were selected and amplified, after which the spacer identity was verified by means of Sanger sequencing.

Final assembly - The sgRNA entry vectors were combined with MultiSite Gateway™ (Thermo Fisher Scientific) with the entry vector pEN-L4-*PAGROI*-SpCas9-T3T-R1 and the destination vector pBbm42GW7 (11) according to the manufacturer's instructions. Correct plasmids were verified by restriction digest with EcoRV.

Base editing vector construction.

virB promoter - The *virB* promoter was cloned with B1A_VIRBLF and B1C_VIRBR (*SI Appendix*, Table S2) and the *A. tumefaciens* EHA105 genomic DNA as template. After purification, PCR products were cut with BsaI and the fragments were ligated into the BsaI site of pGGA-C to generate pGG-A-*PvirB*-C (*SI Appendix*, Figure S5A).

CBE module - DNA of pScI_dCas9-CDA-UL (12) was digested by the ApaI and PvuI and blunted with Q5 polymerase (NEB), thereafter the digest was purified. After the pGGC000 DNA had been cut by KpnI and BamHI, the digest was purified and blunted. The blunted DNA was purified and dephosphorylated with shrimp alkaline phosphatase (Roche) according to the manufacturer's protocol. The blunted pScI_dCas9-CDA-UL DNA was ligated to blunted and dephosphorylated pGGC000 to generate pGG-C-dCas9-CDA-UL-D (*SI Appendix*, Figure S5A). Subsequently, the Gateway entry clone pEN-L4-*PvirB*-dCas9-CDA-UL-T3T-R1 was constructed by Golden Gate cloning of pGG-A-*PvirB*-C, pGG-C-dCas9-CDA-UL-D, and pGG-D-T3T-G with pEN-L4-AG-R1 (*SI Appendix*, Figure S5A). The entry vectors containing the sgRNA were constructed as previously described (*SI Appendix*, Figure S5B) and combined with the

destination vector pBbm42GW7 (11) according to the manufacturer's instructions, except for experiments that included curing.

sacB module - By combining pGG-F-AarI-*sacB*-AarI-G and pGG-A-LinkerIII-F (13) with pEN-R2-AG-L3 (14) through Golden Gate cloning, pEN-R2-*sacB*-L3 was generated (*SI Appendix*, Figure S5C). For base editing combined with curing, the MultiSite Gateway™ reactions were done with the sgRNA entry vectors, pEN-L4-*PvirB*-dCas9-UL-T3T-R1 and pEN-R2-*sacB*-L3, and the destination vector pPm43GW (11) (*SI Appendix*, Figure S5D). The resulting vectors were verified by restriction enzyme digestion.

Multiplexing - We generated a template Scaf-PJ23119 combination with the oligonucleotides CROPGEN568 and CROPGEN569 (*SI Appendix*, Table S2) that was inserted into pJET1.2 (Thermo Fisher Scientific) to yield pJET-Scaf-PJ23119. For the construction of the base-editing system with two sgRNAs, pJET-Scaf-PJ23119 was used as a template for PCR with primers containing two spacers in the four-primer mixture (CROPGEN585-588) as described (15). The purified PCR fragment spacer1-Scaf-PJ23119-spacer2 could then be cloned in pEN-L1-PJ23119-BsaI-*PglpT*-sfGFP-*TrrfB*-BsaI-Scaf-L2 as described to yield pEN-L1-PJ23119-spacer1-Scaf-PJ23119-spacer2-Scaf-L2 (*SI Appendix*, Figure S6C). Vectors are available upon request from <https://gatewayvectors.vib.be/>.

Design of sgRNAs. sgRNAs were designed manually by means of the CLC Workbench 8.1 (Qiagen) or Geneious Prime® 2019.2.3 to introduce stop codons (CRISPR-STOP (16)) 15 to 22 bp 5' of a NGG PAM sequence. Premature stop codons could only be introduced by targeting the codons 5'-CAA-3' (Gln), 5'-CAG-3' (Gln), 5'-CGA-3' (Arg) on the (+) strand or 5'-CCA-3' on the (-) strand (encoding Trp on the (+) strand), because the C→T residue transition would result in the introduction of a stop codon (TAA, TAG, and TGA) at the desired location (16). Depending on the position of the targeted C, the spacer length was adjusted to 18, 20, or 22 bp (12). Specificity and possible off-targets were checked with Geneious using default settings (Geneious "Find CRISPR Sites" plugin with settings: Target = Spacer sequence; PAM Site = NGG; Score against an off-target database = *A. tumefaciens* EHA105 (circular chromosome, NC_003062; linear chromosome, NC_003063; pAtC58, NC_003064; pTiBo542, DQ058764) or *A. rhizogenes* K599 (circular chromosome, NZ_CP019701; linear chromosome, NZ_CP019702; pRi2659, NZ_CP019703); Maximum mismatches allowed against off-targets = 4; Maximum mismatches allowed to be inDels = 0). Only sgRNAs without predicted off-targets were used. All spacers used are provided (*SI Appendix*, Table S3).

Base editing and plasmid curing. Base-editing constructs were transferred to *A. tumefaciens* via heat shock or to *A. rhizogenes* via electroporation. For selection, cells were grown on spectinomycin-containing LB medium or on glucose-spectinomycin-streptomycin—containing AT minimal medium for *A. tumefaciens* and *A. rhizogenes*, respectively. Colony PCR was used to check the base editing in transformants. The target region was amplified with GoTaq® DNA

Polymerase (Promega) or Dreamtaq polymerase (Thermo Fisher Scientific) and appropriate primers (*SI Appendix*, Table S2). Amplicons were purified with HighPrep™ PCR (MAGBIO) or GeneJet PCR purification Kit (Thermo Fisher Scientific). The Sanger sequencing was done by Eurofins Genomics GmbH (Ebersberg, Germany) or LGC Genomics (Berlin, Germany). The chromatograms were analyzed with SnapGene (GSL Biotech) and EditR (17). To obtain plasmid-free strains, edited *Agrobacterium* strains were streak plated on sucrose-containing medium and incubated at 28°C. Next, 20-40 colonies were tested for successful removal of the base-editing plasmid by plating them both on medium +10% (wt/vol) sucrose and medium +10% (wt/vol) sucrose + spectinomycin. Curing was confirmed by colony PCRs with primers CROPGEN577 and CROPGEN578 (*SI Appendix*, Table S2). Base editing at the target site and clone purity were verified by isolation of genomic DNA using Wizard® (Promega). The target region was amplified with Q5® high-fidelity polymerase (New England Biolabs) and sequencing was done as above.

Acetosyringone treatment. The influence of AS on editing was examined by plating agrobacteria on *Agrobacterium* minimal media (AB*) with glucose as carbon source and selection on spectinomycin (18). After transformation, a single colony was grown in liquid AB* overnight, diluted in AB* medium supplemented with 10 µM AS, and grown for 24 h. AB* was used for optimal *PvirB* induction (19). After *PvirB*-dCas9-CDA-UL induction by AS, genomic DNA was extracted from the transformed bacteria and genome editing was analyzed by means of PCR and Sanger sequencing as described above.

Immunoblot assay. Agrobacteria were transformed with the base editor construct and plated on solid LB medium with 100 µg/mL spectinomycin and with or without 10 µM AS. Untransformed EHA101 plated on LB medium was used as a negative control. All colonies from one plate were collected after 3 days in corresponding liquid LB medium, vortexed, diluted until $OD_{600}=1.4$, and subsequently pelleted by centrifugation at 5000g for 10 min. Excess medium was removed, pellets were snap frozen in liquid nitrogen, and stored at -70°C. For protein isolation, pellets were resuspended in 150 µL urea lysis buffer (9 M urea, 50 mM NH_4HCO_3 , pH 7.9) followed by three freeze-thaw cycles in liquid nitrogen (20). Subsequently, lysates were sonicated (Branson probe sonifier output 4, 50% duty cycle, 3×30 s, 1 sec pulses), centrifuged for 10 min at 16,100g (4°C). The protein concentration of the supernatant was determined using a Qubit assay (Thermo Fisher Scientific). A volume of 50 µg total protein was equalized with urea lysis buffer, after which 5× loading buffer was added. The samples were boiled for 5 min and loaded on a 4–20% (wt/vol) TGX gel (Bio-Rad) and run for 25 min at 250 V. A Trans-Blot Turbo Transfer System (Bio-Rad) was used for blotting on 0.2-µm polyvinylidene difluoride membranes. A 1/5000 dilution of a horseradish peroxidase-conjugated Cas9 antibody (ab202580, Abcam) was used. Chemiluminescence was detected with Western Bright ECL (Isogen). Equal loading was inspected by staining of the membrane using Ponceau S (Sigma-Aldrich).

MMS susceptibility assay. For testing the susceptibility of EHA105, EHA105-*recA(Q26*)*, and EHA105-*recA(Q178*)* to MMS, a single loop of bacteria freshly grown on YEP plates (5 g/L yeast extract, 10 g/L peptone, 5 g/L NaCl, 8 g/L agar, pH 6.8, and 100 µg/mL rifampicin) was used to inoculate a 5-mL overnight culture in YEP medium at 28°C in a shaker at 200 rpm. The following morning, 1 mL of the overnight culture was added to 19.2 mL in a 250-mL Erlenmeyer and incubated at 28°C in a shaker at 200 rpm for 4 h, resulting in an OD₆₀₀ of 0.50-0.51 for all strains. A dilution series was made to 10⁻⁵ in sterile water in a 96-well plate. Of each dilution, a 3-µL drop was put on a replica plater with YEP medium containing 0.005% (vol/vol) MMS or mock and grown for 24 h at 28°C.

B104 maize transformation. EHA105, EHA105 *recA(Q26*)*, and EHA105 *recA(Q178*)* were transformed with pXBb7-SI-UBIL (21). Agrobacteria were cocultivated with immature embryos of the maize inbred B104 as described (22). Embryos were isolated from three different cobs of independent plants 12 days after pollination. Briefly, agrobacteria were grown on a fresh spectinomycin-containing YEP plate for 2 days at 28°C. Cells were resuspended in 5 ml of infection medium (22) with 100 µM AS in a 50-ml tube and incubated for 2–5 h at room temperature. Subsequently, the bacteria were diluted to an OD₅₅₀ = 0.3–0.4 and 1 ml of agrobacteria was added to 20-30 embryos in an Eppendorf tube that was gently inverted 20 times before a 5 min rest in the dark. Infected embryos were plated on cocultivation medium (22) and incubated for 3 days, transferred to resting media (22) for another 4 days before GUS analysis of transient expression.

Histochemical X-Gluc assay. The 5-bromo-4-chloro-3-indolyl-β-D-glucuronide (X-Gluc) assay was done as described (22, 23). Briefly, embryos were placed in a 90% (vol/vol) acetone solution for 30 min at 4°C. Next, the acetone was replaced by a fresh phosphate buffer (50 mM Na₂HPO₄, 50 mM NaH₂PO₄, pH 7, and 0.01% [vol/vol] Triton X-100) under gentle agitation for 15 min at room temperature. Next, the buffer was replaced by 2 mM potassium ferri/ferrocyanide-containing phosphate buffer and vacuum infiltrated for 10 min and subsequently incubated at 37°C for 30 min in the dark. Finally, samples were transferred to 2 mM potassium ferri/ferrocyanide-containing phosphate buffer supplemented with 3 mM X-Gluc, vacuum infiltrated for 10 min, and incubated in the dark at 37°C. All embryos scutellum-side up were imaged with a M80 binocular microscope (Leica), and the GUS activity-positive area was calculated by means of ImageJ with a custom-made script (24). Statistics were analyzed and boxplots were constructed with Graphpad Prism (version 8 for MacOS).

Carrot disk virulence assay. The pathogenicity of all *A. rhizogenes* mutants generated by the base-editing system was tested in an *in vitro* carrot disk bioassay with modifications (25). Briefly, carrots were surface-sterilized and cut into 0.5-cm thick pentagon sized disks and placed on 0.9% (wt/vol) agar plates with upward-facing root apical directions. *A. rhizogenes* strains

K599, K599-*rolB*(R31*), K599-*rolB*(W167*), K599-*rolC*(Q40*), and K599-*orf13*(Q29*) grown overnight in liquid YEP medium were diluted to an $OD_{600} = 0.072$ ($\sim 7.5 \times 10^7$ colony-forming units). Of this suspension, 10 μ L was used to inoculate each carrot disk, whereas the mock controls were inoculated with 10 μ L of liquid YEP. The inoculated carrot disks were placed in an incubator at 25°C and 80 μ mol m⁻² s⁻¹ light for 24 h. Hairy root growth was recorded over a period of 8 weeks. Statistical analyses were done and graphs were constructed with GraphPad Prism (version 8 for MacOS).

Whole-genome sequencing. The whole genomes of the *A. tumefaciens* EHA105 and *A. rhizogenes* K599 strains were sequenced by means of combined in-house Illumina short-read sequencing (Miniseq Illumina NGS platform) and Nanopore long-read sequencing (MinION Oxford Nanopore Technologies). Total genomic DNA was extracted from the two strains with the E.Z.N.A bacterial genomic DNA kit (Omega Biotek) according to the manufacturer's instructions. For the Illumina sequencing, the library was prepared with the Nextera Flex DNA library kit. The average DNA fragment lengths (750 bp) were evaluated with a Bioanalyzer 2100 and a High Sensitivity Kit (Agilent Technologies) and the concentration was determined with Qubit (Thermo Fisher Scientific). Long reads of the reference genome were obtained by means of the MinION sequencer (Flowcell R9.4.1; Oxford Nanopore Technologies) and the Rapid Sequencing Barcoding Kit, according to the manufacturer's instruction, whereas Guppy (v3.1.5) was used for the Nanopore basecalling (26). The adapters of the Illumina and Nanopore reads were trimmed with Trimmomatic (v0.36.5) (27) and Porechop (v0.2.4) (28), respectively. Next, a hybrid assembly of the reference genomes was obtained with Unicycler (v0.4.8.0) (29) and evaluated by means of Bandage (v0.8.1) (30). The bioinformatics were analyzed by the usegalaxy.eu platform (31). The final K599 and EHA105 genomes were annotated with PROKKA (v1.13+) (32) and RASTtk (33), respectively, on the PATRIC platform (v3.6.3) based on the available annotation of *A. rhizogenes* K599 (circular chromosome, NZ_CP019701; linear chromosome, NZ_CP019702; pRi2659, NZ_CP019703) and *A. tumefaciens* C58 (circular chromosome, NC_003062; linear chromosome, NC_003063; pAtC58, NC_003064) and pTiBo542 (DQ058764). Single nucleotide polymorphism (SNPs) between EHA105 and the reference genome were determined as described below, whereas a list of unique genes between pEHA105 and pTiBo542 was created with Roary (v3.13.0) (34). Genome maps were drawn by means of EasyFig (35).

Genome-wide off-target analysis. To evaluate the off-target effects of the base-editing system post curing, total genomic DNA was extracted from the cured strains EHA105-*recA*(Q26*), EHA105-*recA*(Q178*), K599-*rolB*(R31*), K599-*rolC*(Q40*), and K599-*orf13*(Q29*) with the E.Z.N.A. bacterial genomic DNA kit (Omega Biotek) according to the manufacturer's instructions. The mutant strains were sequenced with the MiniSeq Illumina NGS platform and sequencing reads were processed as described above. Three different variant calling tools, Genome analysis tool kit (GATK) HaplotypeCaller V4.1.7.0 (36), Freebayes V0.9.21 (37), and the function mpileup from BCFtools v.1.9 were used to identify single nucleotide variants

(SNVs) between EHA105 and K599 and the respective reference genomes. Similarly, the DNA sequencing reads from the mutant lines were used to identify SNVs compared with the assembled genomes of the laboratory parent strains of K599 and EHA105. The accuracy of the Illumina sequencing platform experiment was 99.97% and we maintained a call read threshold of 90% for a nucleotide to be labelled a SNV. In the analysis pipelines, quality-trimmed reads were mapped to the reference genome using BWA-mem (38). The resulting SAM files were parsed into BAM files with samtools 'view'. The BAM files were sorted and reads marked for duplicates with PICARD tools (<http://broadinstitute.github.io/picard/>) prior to SNV calling with the above-mentioned tools. To filter out the raw variants and to keep only the variants with high confidence, we used SnpSift (39) in the mpileup, VCFtools (40) for the Freebayes and GATK (41) for the GATK-HaplotypeCaller pipelines. To predict the effect of the called variants SnpEff (42) was used on the filtered variant calling files. To manually confirm and evaluate the identified SNVs, we visualized the filtered SNVs in the produced VCF files with the Integrated Genome Viewer (IGV) (43). For statistical analyses of upstream nucleotide substrate preference, percentages were normalized using the arcsine square root function and statistics was performed with GraphPad Prism (version 8 for MacOS). Motif analyses for the substrate preference of unguided dCas9-CDA-UL in *E. coli* (12) was subject to a similar analysis as described for base-edited *Agrobacterium* spp. mutants.

SUPPLEMENTARY FIGURES

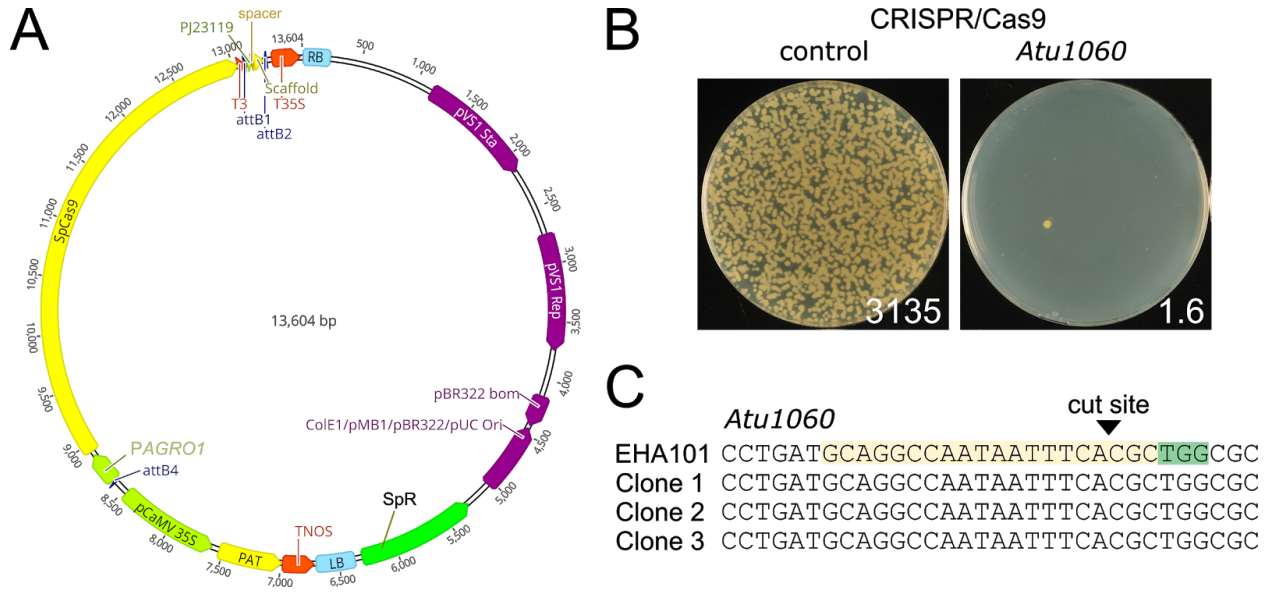


Fig. S1. Lethality of CRISPR/Cas9 activity in *A. tumefaciens* EHA101 when targeting a chromosomal locus. (A) Vector used for CRISPR/Cas9 gene editing in *A. tumefaciens*. *PAGRO1*, constitutive promoter; SpCas9, *Streptococcus pyogenes* Cas9 nuclease; T3, terminator of the RNA polymerase III of bacteriophage T3; PJ23119, constitutive synthetic promoter; attB1, attB2, and attB4, Gateway recombination sites; PAT, phosphinothricin acetyltransferase; LB, left border; RB, right border; SpR, spectinomycin resistance. (B) Representative pictures of *A. tumefaciens* EHA101 cells transformed with either a vector containing a sgRNA targeting the chromosomal gene *Atu1060* or a control without functional spacer and plated on selective medium with spectinomycin. Average number of colonies in a single transformation experiment is shown ($n = 3$). (C) Sequencing results of the *Atu1060* locus in three random surviving colonies. No hallmarks of DNA repair are visible. PAM and protospacer are highlighted in green and yellow, respectively. Triangle indicates predicted Cas9 cut site.

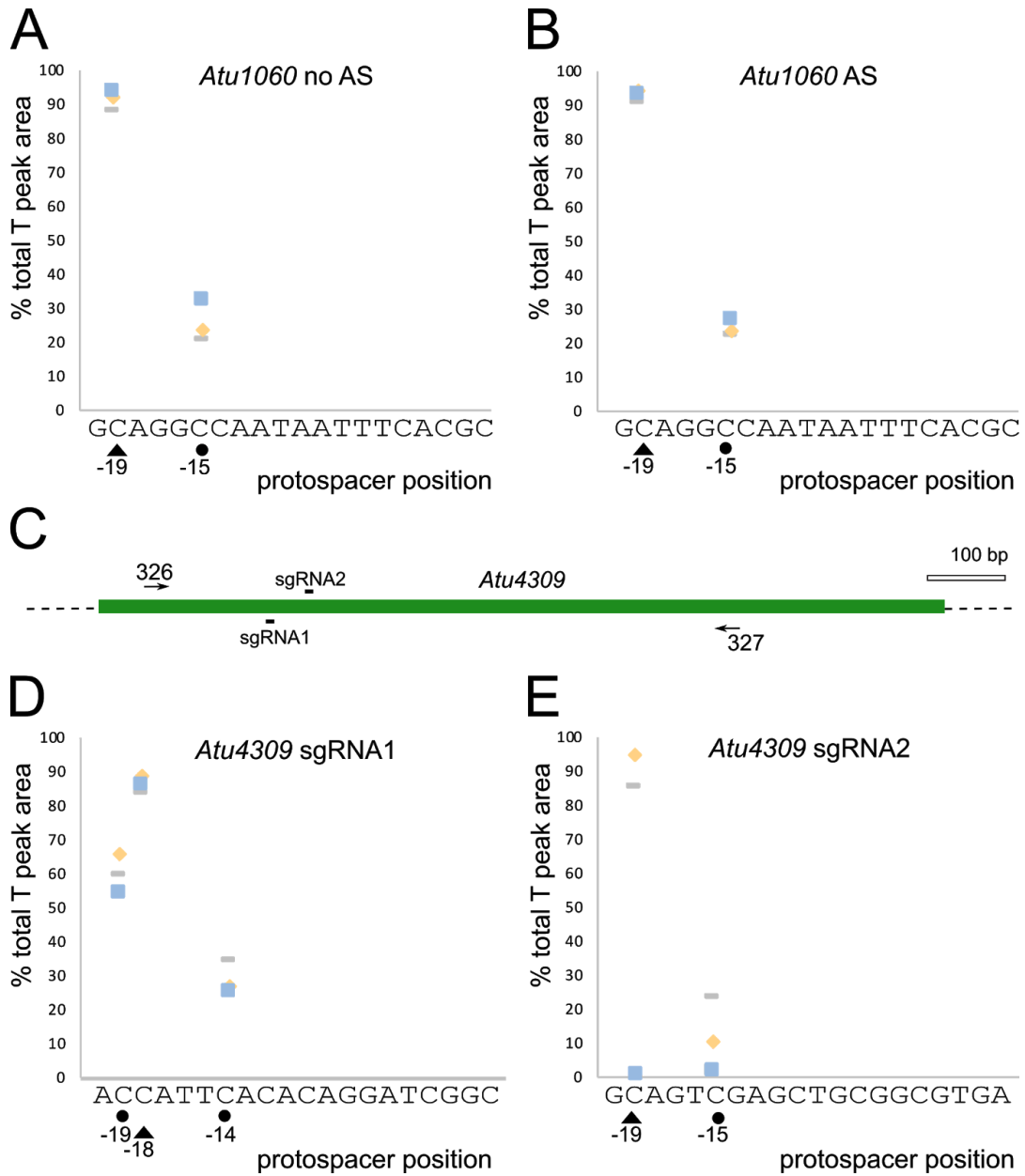


Fig. S2. Efficient base editing of *A. tumefaciens* EHA101. (A) and (B) Quantification of the C→T editing at the *Atu1060* locus without (A) or with acetosyringone treatment (B). The percentage of the total peak area of the Sanger sequencing reads is shown at the different protospacer positions when an edit significantly differs from noise. Each series of dots represents an independent colony after transformation ($n = 3$). Solid triangles and solid circles denote targeted C and bystander C, respectively, with the numbering indicating positions relative to the PAM. (C) The *Atu4309* genomic locus. Locations of the protospacer used for the sgRNA are indicated together with the position of the primers used for genotyping. (D) and (E) Quantification of the C→T editing at the *Atu4309* locus for sgRNA1 (D) or sgRNA2 (E). The same symbol was used for the same strains.

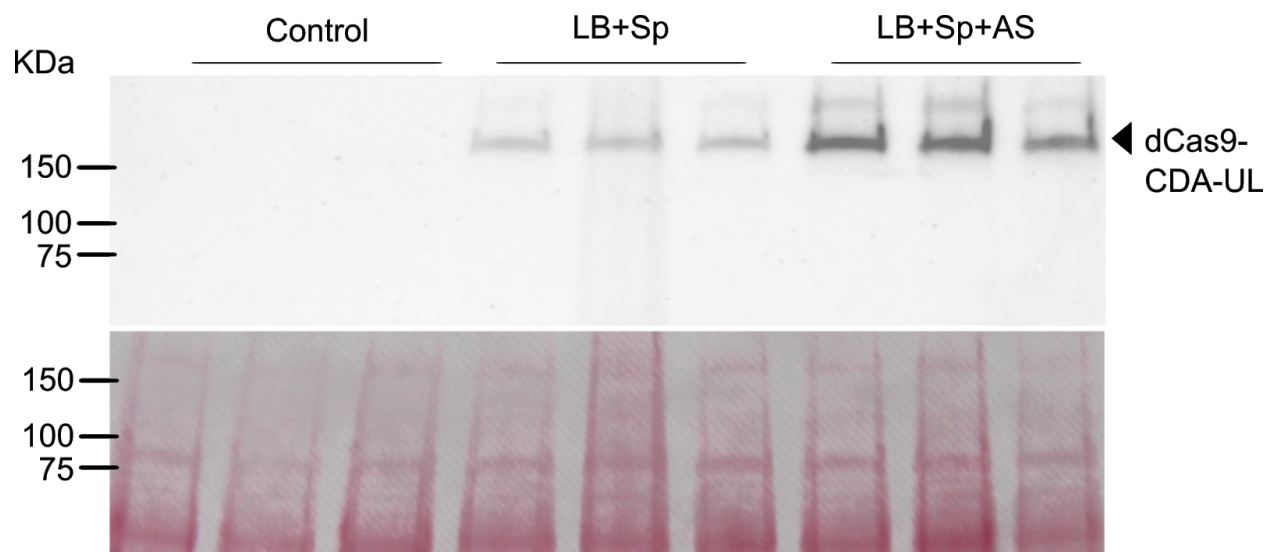


Fig. S3. Leaky expression of *PvirB* in *A. tumefaciens* EHA101. Immunoblot with anti-Cas9 antibody showing dCas9-CDA-UL levels in three biological repeats. *Agrobacterium* cells were transformed with the base editor construct targeting *Atu1060* and plated on LB medium with spectinomycin (Sp) and with or without 10 μ M acetosyringone (AS). All colonies of a plate were collected after 3 days as one biological repeat. Freshly plated (non-transformed) EHA101 was used as a negative control. Membranes were stained with Ponceau S to inspect equal loading.

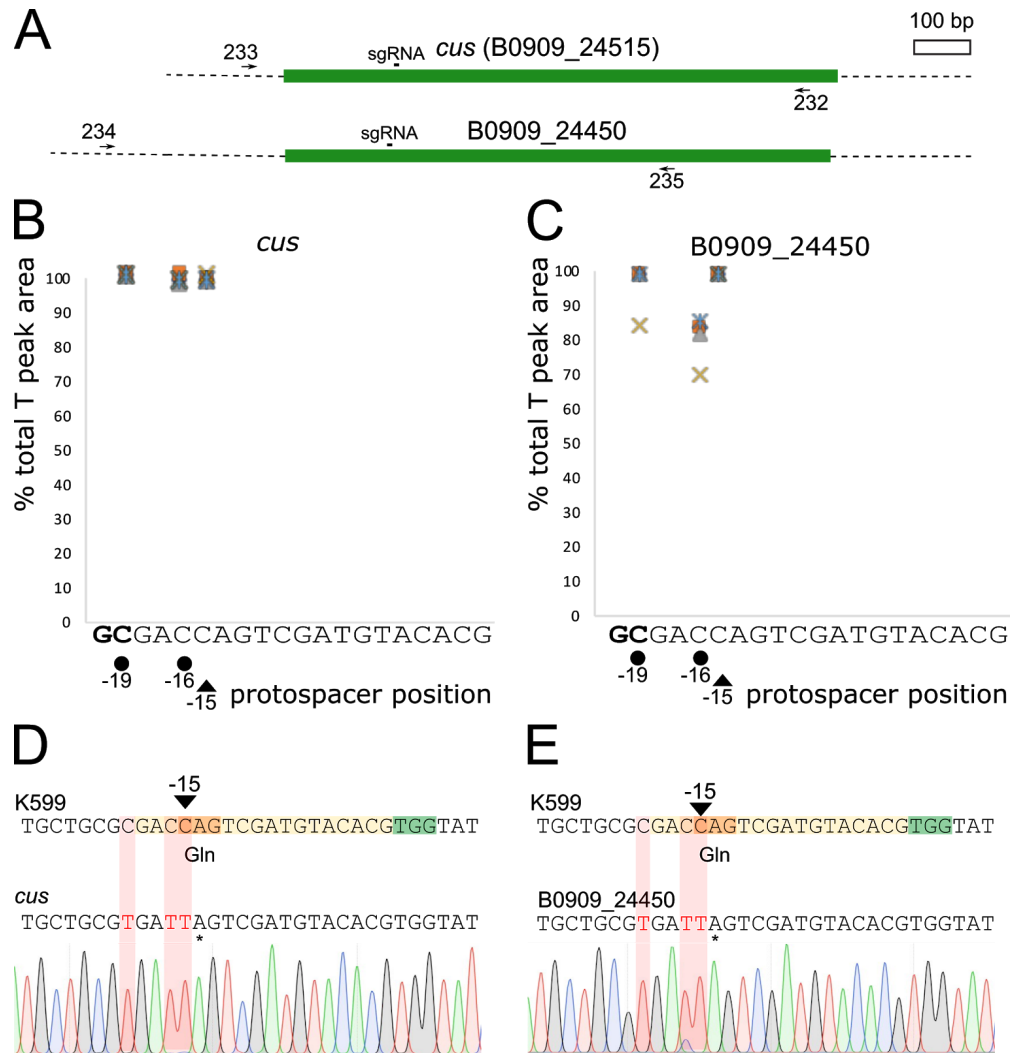


Fig. S4. Efficient base editing in *A. rhizogenes*. (A) Cucumopine synthase-encoding gene (*cus*, B0909_24515) and the B0909_24450 genomic locus in the K599 genotype. Locations of the protospacer used are indicated together with the position of the primers used for genotyping. (B) and (C) Quantification of the C→T editing at the *cus* (B) and B0909_24450 genomic loci (C). The percentage of the total peak area of the Sanger sequencing reads is shown at the different protospacer positions when an edit significantly differs from noise. Each series of dots represents an independent colony after transformation ($n = 5$). Solid triangles and solid circles denote targeted C and bystander C, respectively, with the numbering indicating positions relative to the PAM. Nucleotides in bold represent bases upstream of the selected spacer. The same symbol was used for the same strains. (D-E) Base editing outcomes. *Upper*, sequences obtained from K599 are shown for *cus* (D) and B0909_24450 (E) with the PAM (green), protospacer (yellow), and target codon (orange). The targeted C is indicated with a triangle, together with the position relative to the PAM. *Lower*, Representative sequences obtained after transformation and without AS induction are shown together with the chromatogram. Edited bases are highlighted in red, the relevant codons are translated, and an asterisk indicates a stop codon. Gln, glutamine.

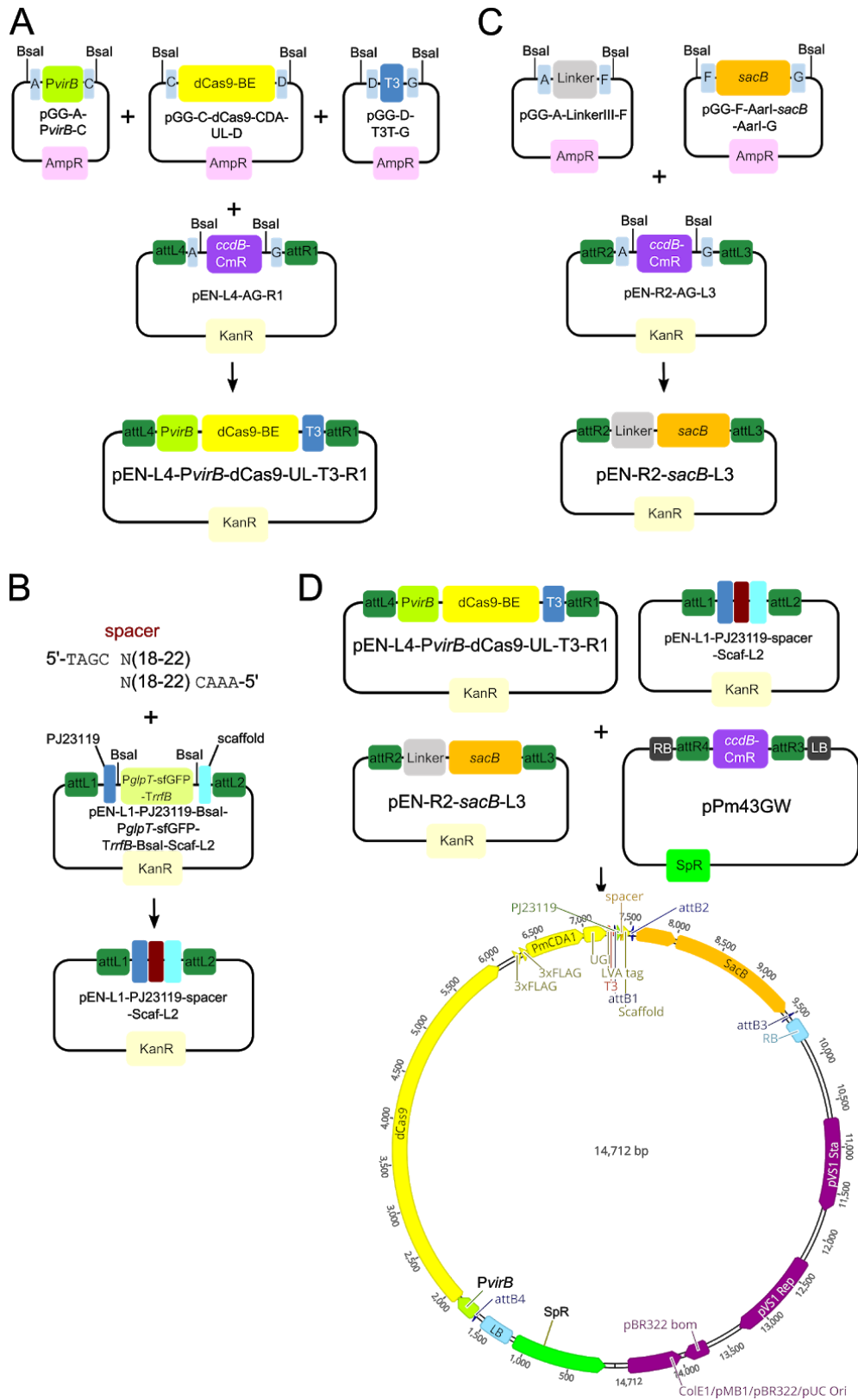


Fig S5. Overview of the construction of the base-editing vector for *Agrobacterium* spp.

Fig S5 (continued). Overview of the construction of the base-editing vector for *Agrobacterium* spp. (A) Construction of the CBE module using Golden Gate cloning. (B) Spacer cloning procedure. Two oligonucleotides are synthesized with 4-bp overhangs for BsaI cloning and contain a spacer of 16 to 22 nucleotides. Annealed oligonucleotides are cloned in a shuttle vector that contains the PJ23119 and sgRNA scaffold module. (C) Cloning of the *sacB* module using Golden Gate. (D) Combination of all modules using MultiSite Gateway cloning resulting in a final clone ready for use in *Agrobacterium* spp.. *PvirB*, promoter fragment of the pEHA105 *virB* gene; dCas9-BE, fusion of nuclease-dead Cas9; PmCDA1, *Petromyza marinus* cytidine deaminase; UGI, uracil DNA glycosylase inhibitor; LVA, protein degradation tag; Scaf, sgRNA scaffold; T3, terminator of the RNA polymerase III of bacteriophage T3; *sacB*, levansucrase; A-G, Golden Gate cloning overhangs; attL1, attL2, attL3, attL4, attR1, attR2, attR3, and attR4, Gateway recombination sites; LB, left border; RB, right border; *ccdB-CmR*, *ccdB* toxin-chloramphenicol resistance cassette; AmpR, ampicillin resistance; KanR, kanamycin resistance; SpR, spectinomycin resistance.

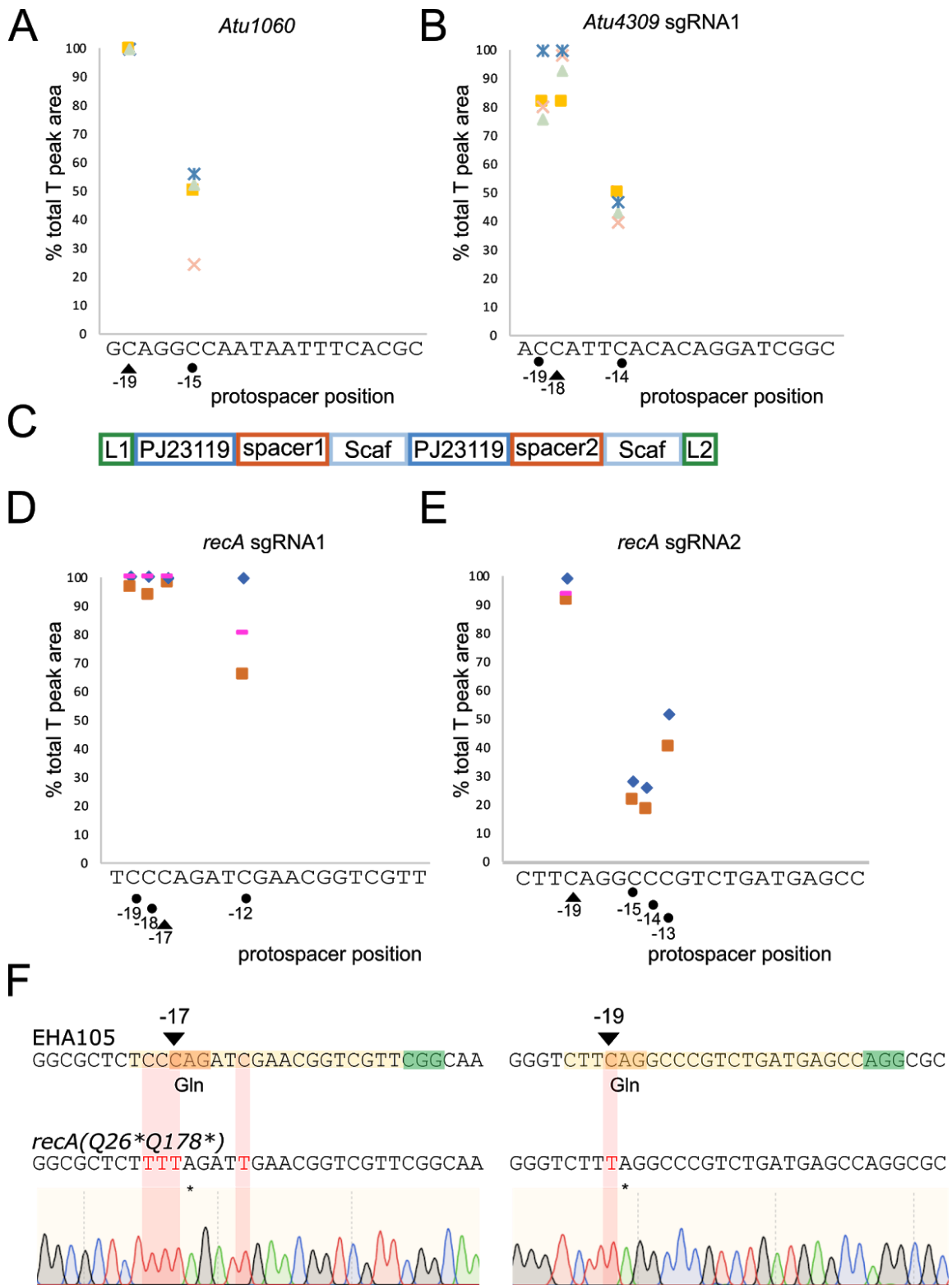


Fig. S6. Efficient single and multiplexed base editing in the presence of *sacB*.

Fig. S6 (continued). Efficient single and multiplexed base editing in the presence of *sacB*. (A) and (B) Quantification of the C→T editing at the *Atu1060* (A) and *Atu4309* (B) genomic loci in colonies after transformation with the *sacB*-containing construct and before curing. The percentage of the total peak area of the Sanger sequencing reads is shown at the different protospacer positions when an edit significantly differs from noise. Each series of dots represents an independent colony after transformation ($n = 4$). Solid triangles and solid circles denote targeted C and bystander C, respectively with the numbering indicating positions relative to the PAM. (C) Multiplexing construct. Two sgRNA modules with different spacers were cloned in tandem. (D) and (E) Quantification of the C→T editing at the *recA* locus after transformation with two sgRNAs with the *sacB*-containing construct ($n = 3$). The same symbol was used for the same strains. (F) Base editing outcome after multiplexing and curing. *Upper*, *recA* sequences at both targets obtained from EHA105 are shown with the PAM (green), protospacer (yellow), and target codon (orange). The targeted C is indicated with a triangle, together with the position relative to the PAM. *Lower*, Representative sequences obtained after curing are shown together with the chromatogram. Edited bases are highlighted in red, relevant codons are translated, and an asterisk indicates a stop codon. Gln, glutamine.

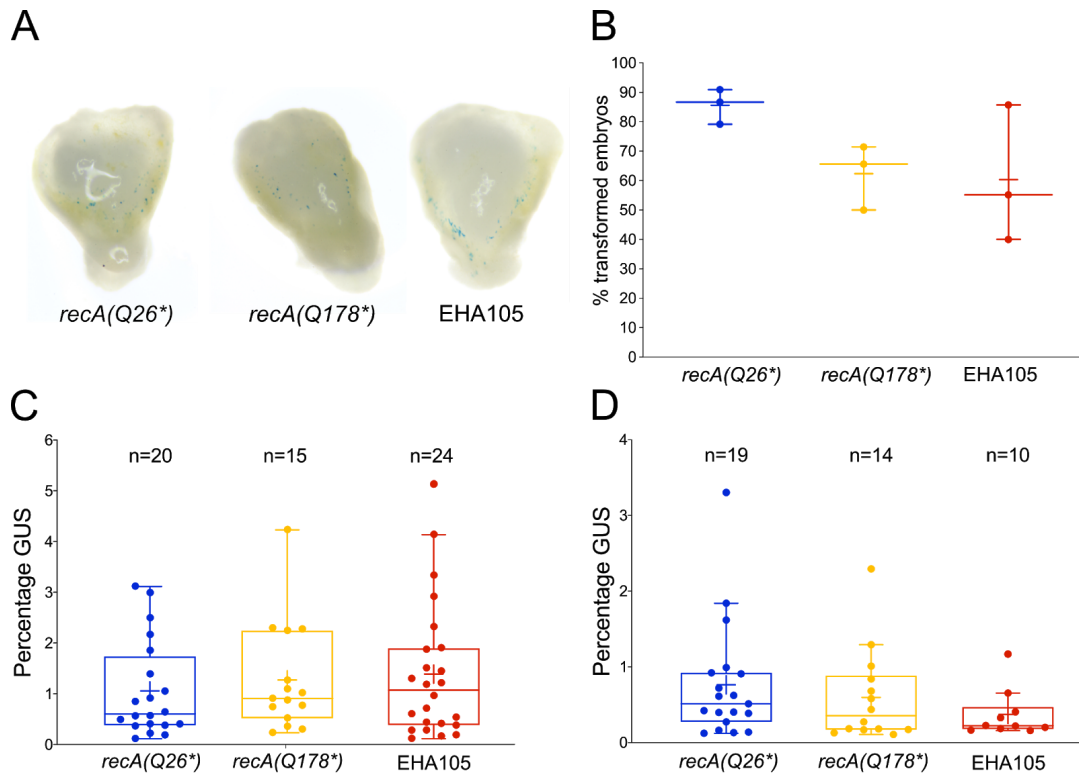


Fig. S7. Lack of impact of EHA105 *recA* mutants on the maize transformation efficiency. (A) Representative images of B104 immature embryos transiently transformed with EHA105 or with base-edited strains carrying the pZmUBI-1::gus reporter construct, 7 days after cocultivation. (B) Fraction of embryos successfully transformed with each strain. Embryos were scored as transformed when more than 0.1% of the imaged area colored blue. In each independent experiment ($n = 3$), embryos derived from a single infected ear were divided over the different strains. No statistically significant differences were observed between the EHA105 parent strain and the EHA105 *recA* mutants (one-way ANOVA with Tukey's multiple comparisons test). (C) and (D) Percentage of the embryo surface scoring positive for GUS. Plotted are values for embryos from a single ear infected with the different strains. No statistically significant differences were observed between the EHA105 parent strain and the EHA105 *recA* mutants (Kruskal-Wallis test and Dunn's multiple comparisons test, $P > 0.05$). Boxplots show medians as center lines and means as crosses; the box limits indicate the 25th and 75th percentiles; whiskers extend to 1.5 times the interquartile range. All data points are solid circles.

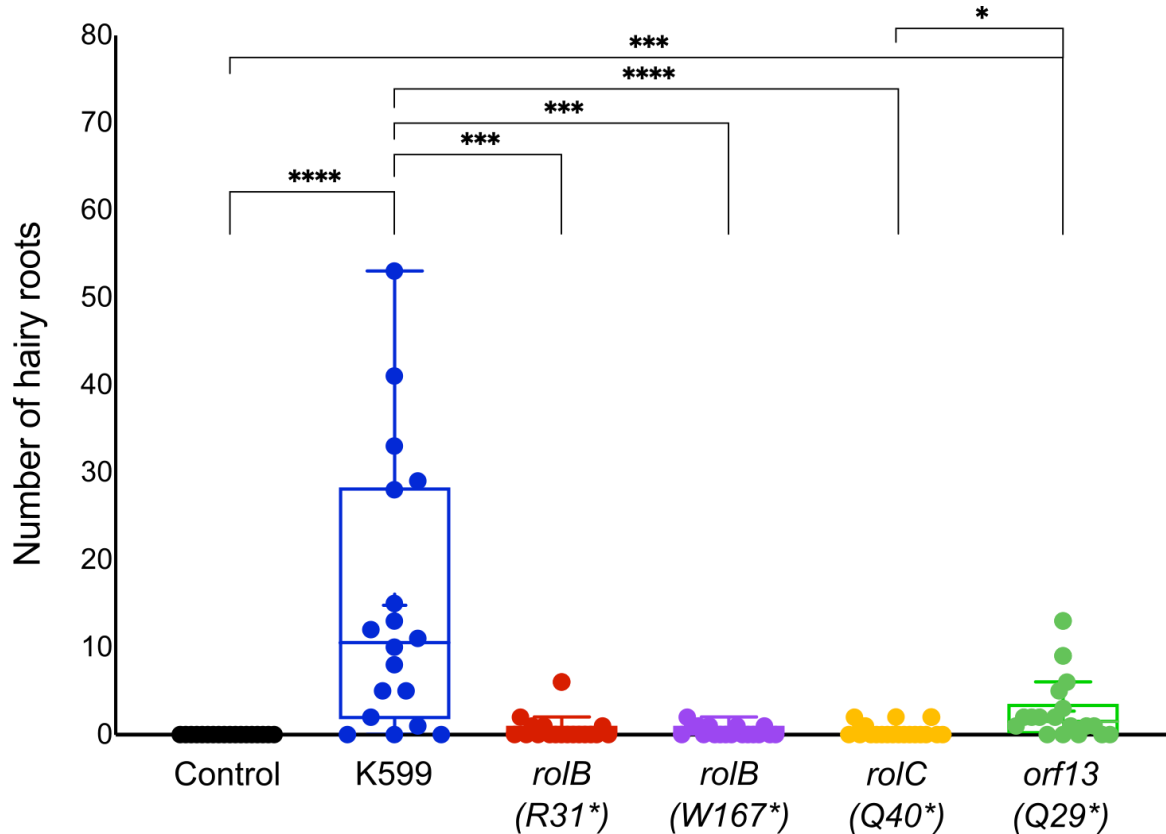


Fig. S8. Hairy root endpoint analysis after 54 days. For each strain, 18 carrot disks were inoculated per treatment group. As a control, disks were inoculated with sterile YEP medium. Boxplots show medians as center lines and means as crosses; the box limits indicate the 25th and 75th percentiles; whiskers extend to 1.5 times the interquartile range. All data points are solid circles. Asterisks mark significant differences with * $P < 0.05$, ** $P < 0.01$, *** $P < 0.001$ and **** $P < 0.0001$ (Kruskal-Wallis test and Dunn's multiple comparisons test).

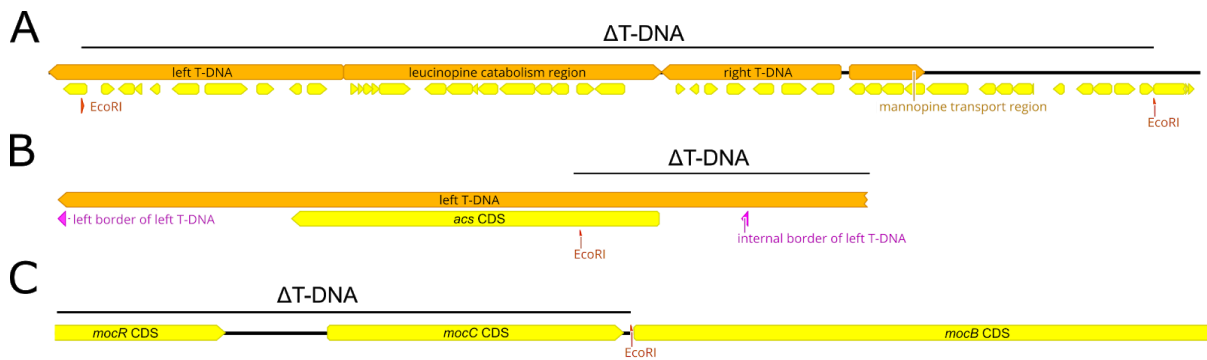


Fig. S9. Detailed scheme of the deleted pTiBo542 T-region in pEHA105. (A) Overview of the deleted T-region consisting of the left T-DNA, the leucinopine catabolism region, the right T-DNA, and the mannopine transport region. The EcoRI sites used for allelic replacement (1) are highlighted. (B) Detailed view of the left T-region. The remaining left border of the left T-DNA is highlighted. *acs*, agrocinnopine synthase-encoding gene. (C) Detailed view of the 3' part of the deleted region. *mocR*, *mocC*, and *mocB*, mannityl opine catabolism-encoding genes.

Table S1. Bacterial strains and plasmids. For the bacterial strains, the features, such as antibiotic resistances, plasmid harbored, and source are detailed. For plasmids, antibiotic resistances, the functional roles, and the source are provided. StR, streptomycin resistance; KmR, kanamycin resistance; RifR, rifampicin resistance; CmR, chloramphenicol resistance; SpR, spectinomycin resistance;; AmpR, ampicillin resistance; pTiBo542- Δ T-DNA, plasmid harbored by *A. tumefaciens* EHA105 with deleted T-DNA region; pRi2659, plasmid harbored by *A. rhizogenes* K599; dCas, dCas9; CDA, cytidine deaminase; UL, fusion construct of UGI and LVA.

Name	Features	Source
Bacterial strain		
<i>E. coli</i> DH5 α		Thermo Fisher
<i>E. coli</i> DB3.1		Invitrogen
<i>A. tumefaciens</i> EHA101	KmR, RifR, A136, pTiBo542- Δ T-DNA	(1)
<i>A. tumefaciens</i> EHA105	RifR, A136, pTiBo542- Δ T-DNA	(2)
<i>A. rhizogenes</i> NCPPB2659 (K599)	StR, CmR, pRi2659	NCPPB
<i>A. tumefaciens</i> EHA105- <i>recA</i> (Q26*)		This work
<i>A. tumefaciens</i> EHA105- <i>recA</i> (Q178*)		This work
<i>A. rhizogenes</i> NCPPB2659- <i>rolB</i> (R31*)		This work
<i>A. rhizogenes</i> NCPPB2659- <i>rolB</i> (W167*)		This work
<i>A. rhizogenes</i> NCPPB2659- <i>rolC</i> (Q40*)		This work
<i>A. rhizogenes</i> NCPPB2659- <i>orf13</i> (Q29*)		This work
Plasmid		
pSEVA421-Cas9-tracrRNA	Source of SpCas9, KmR	(8)
pScI_dCas9_CDA_UL	Source of dCas9-CDA-UL, CmR	(12)
pPZP200	Source for <i>PAGROI</i>	(5)
pPGW	Source of <i>ccdB</i> -CmR, SpR	(21)
pGGA000, pGGB000, pGGC000	Empty Golden Gate entry vectors, AmpR	(6)
pGGD-G, pGGA-C	Empty Golden Gate entry vectors, AmpR	This work
pGG-A- <i>PAGROI</i> -B	Constitutive promoter, AmpR	This work
pGG-A-P <i>virB</i> -C	pTiBo542 <i>virB</i> promoter, AmpR	This work
pGG-C-SpCas9-D	SpCas9 nuclease, AmpR	This work
pGG-C-dCas9-CDA-UL-D	Target-AID base editor, AmpR	This work
pGG-D-T3T-G	Bacterial terminator, AmpR	This work
pGG-F-AarI- <i>sacB</i> -AarI-G	<i>sacB</i> module, AmpR	(13)
pGG-A-LinkerIII-F, pGG-B-Linker-C	Linker, AmpR	(6, 13)
pEN-L4-AG-R1, pEN-L1-AG-L2, pEN-R2-AG-L3	Empty MultiSite Gateway entry clones, KmR	(9, 14)
pJET1.2	PCR cloning vector, AmpR	Thermo Fisher
pJET-Scaf-PJ23119	PCR template for multiplexing, AmpR	This work
pEN-L1-PJ23119-BsaI-BsaI-Scaf-L2	Shuttle cloning vector for sgRNA, KmR	This work
pEN-L1-PJ23119-BsaI- <i>ccdB</i> -CmR-BsaI-Scaf-L2	Shuttle cloning vector for sgRNA, KmR	This work
pEN-L1-PJ23119-BsaI-P <i>glpT</i> -sfGFP- <i>TrrfB</i> -BsaI-Scaf-L2	Shuttle cloning vector for sgRNA, KmR	This work
pEN-L4- <i>PAGROI</i> -SpCas9-T3T-R1	MultiSite Gateway entry clone, KmR	This work

pEN-L4-PvirB-dCas9-CDA-UL-T3T-R1	MultiSite Gateway entry clone, KmR	This work
pEN-R2-sacB-L3	MultiSite Gateway entry clone, KmR	This work
pBbm42GW7	Destination vector, SpR	(11)
pPm43GW	Destination vector, SpR	(11)
pXBb7-SI-UBIL	Expression vector, SpR	(21)

Table S2. Oligonucleotides used for the construction of sgRNA for base-editing applications, cloning of base-editing constructs, genotyping of base-edited *Agrobacterium* spp. strains, confirmation of curing of base-edited *Agrobacterium* spp. strains, and multiplexing applications. Golden Gate overhangs are in bold and BsaI recognition sites are underlined.

Name	Sequence (5'-3')	Description
sgRNA cloning		
CROPGEN318	TAGCGCAGGCCAATAAATTT CACGC	<i>Atu1060</i>
CROPGEN319	AAACGCGTGAAATTATTGGCCTGC	<i>Atu1060</i>
CROPGEN322	TAGCACCATT CACACAGGATCGGC	<i>Atu4309</i> sgRNA1
CROPGEN330	AAACGCCGATCCTGTGTGAATGGT	<i>Atu4309</i> sgRNA1
CROPGEN324	TAGCGCAGTCGAGCTGCGGCGTGA	<i>Atu4309</i> sgRNA2
CROPGEN331	AAACTCACGCCG CAGCTCGACTGC	<i>Atu4309</i> sgRNA2
CROPGEN496	TAGCTCCCAGATCGAACGGT CGTT	<i>recA (Atu1874)</i> sgRNA1
CROPGEN497	AAACAACGACCGTT CGATCTGGGA	<i>recA (Atu1874)</i> sgRNA1
CROPGEN498	TAGCCTTCAGGCCCGTCTGATGAGCC	<i>recA (Atu1874)</i> sgRNA2
CROPGEN499	AAACGGCTCATCAGACGGGCTGAAG	<i>recA (Atu1874)</i> sgRNA2
PHP-221	TAGCGACCAGT CGATGTACACG	<i>cus</i> (B0909_24515) and B0909_24450
PHP-222	AAACCGTGTACATCGACTGGTC	<i>cus</i> (B0909_24515) and B0909_24450
PHP-239	TAGCCACGAGATCTC ACAAAAGCC	<i>rolB</i> (B0909_24535) sgRNA1
PHP-240	AAACGGCTTTTGTGAGATCT CGTG	<i>rolB</i> (B0909_24535) sgRNA1
PHP-282	TAGCGCCAAGCAATGTTGTGAGCA	<i>rolB</i> (B0909_24535) sgRNA2
PHP-283	AAACTGCTCACAACAT TGCTTGGC	<i>rolB</i> (B0909_24535) sgRNA2
PHP-241	TAGCTCCAGAGCGCCTCAA AGGAG	<i>rolC</i> (B0909_24530)
PHP-242	AAACCTCCTTTGAGGCGCTCT GGA	<i>rolC</i> (B0909_24530)
PHP-243	TAGCCTCAGCTTGT TAAATGTGG	<i>orf13</i> (B0909_24525)
PHP-244	AAACCCACATTAACA AGCTGA	<i>orf13</i> (B0909_24525)
Cloning		
AgroPromo1F	AAGTGAAGCTTGGTCTCAACCTCACGAACCCAGTGGACATAAGC	Constitutive promoter
AgroPromo1R	GCGAGAATTCGGTCTCATGTTGATGTTAACTTTGTTTTAGGGC	Constitutive promoter
SEVA421Cas9F	AGAAGTGAAGCTTGGTCTCAGGCTCCATGGATAAGAAATACTCAATAGGC	SpCas9
SEVA421Cas9R	AGGGCGAGAATTCGGTCTCACTGATCAGTCACCTCCTAGCTG	SpCas9
D_Stop_T3Ter_GF	TCAGAATAAGCAAACCCCTTGGGTTCCCTCTTTAGGAGTCTGAGGGGTTTTTTGCA	T3 terminator
D_Stop_T3Ter_GR	ATACTGCAAAAAACCCCTCAGACTCCTAAAGAGGGAACCCAAGGGGTTGCTTATT	T3 terminator
B1A_VIRBLF	TTTTGGTCTCAACCTGTTGACCGATCCGTCTTGCG	<i>virB</i> promoter

BIC_VIRBR	TTTTGGTCTCAAGCCTCTCCTTAGCTCGCAACTAACAC	<i>virB</i> promoter		
J23119B1B1ScF	ACCT TTGACAGCTAGCTCAGTCCTAGGTATAATGCTAGCAGAGACCC GGGATGGTCTCAGTTTTAGAGCTAGAAATAGCAAGTTAAAAATAAGGC TAGTCCGTTATCAACTTGAAAAAGTGGCACCGAGTCGGTGCTTTTTT T	PJ23119-BsaI-BsaI-scaffold		
J23119B1B1ScR2	ATAC AAAAAAGCACCAGCTCGGTGCCACTTTTTCAAGTTGATAACG GACTAGCCTTATTTAACTTGTATTTCTAGCTCTAAAAC TGAGACC ATCCCCGGTCTCTGCTAGCATTATACCTAGGACTGAGCTAGCTGTCA A	PJ23119-BsaI-BsaI-scaffold		
ccdBAgroF	ATGCTAGCTGAGACCGTCGACTTATATTC	<i>ccdB</i> -CmR		
ccdBAgroR	TCTAAAAC TGAGACC CGGCCGCATTAGG	<i>ccdB</i> -CmR		
CROPGEN254	TGT TAGC GGAGACC GAAAGT GAAACGTGATTTTCATGCC	<i>PglpT</i> -sfGFP- <i>TrrfB</i>		
CROPGEN255	TGT AAAC AGAGACC TCTATA AAACGCAGAAAGGCCACC	<i>PglpT</i> -sfGFP- <i>TrrfB</i>		
CROPGEN568	GTTTTAGAGCTAGAAATAGCAAGTTAAAAATAAGGCTAGTCCGTTATC AACTTGAAAAAGTGGCACCGAGTCGGTGCTTTTTTTTTGACAGCTAG CTCAGTCCTAGGTATAATGCTAGC	Scaffold-PJ23119 generation	PCR	template
CROPGEN569	GCTAGCATTATACCTAGGACTGAGCTAGCTGTCAAAAAAAGCACC GACTCGGTGCCACTTTTTCAAGTTGATAACGGACTAGCCTTATTTTA ACTTGCTATTTCTAGCTCTAAAAAC	Scaffold-PJ23119 generation	PCR	template
Genotyping				
CROPGEN320	AAATGGCCGACTTCCGTAAC	<i>Atu1060</i>		
CROPGEN321	CGACCACCAGAACGGAAAAAC	<i>Atu1060</i>		
CROPGEN326	ATTTGCGCCATGACCTCTCC	<i>Atu4309</i>		
CROPGEN327	AGGATCGCCTTCTTGACCAG	<i>Atu4309</i>		
CROPGEN504	GCTCAGCCTTGCGAAATGAG	<i>recA</i> (<i>Atu1874</i>)		
CROPGEN505	TTCGACTTGAGATCGAGGC	<i>recA</i> (<i>Atu1874</i>)		
CROPGEN579	GGTTTATGCCCGCAAGCTC	<i>recA</i> (<i>Atu1874</i>)		
CROPGEN580	CCATTCTGCAGGAAGCGGT	<i>recA</i> (<i>Atu1874</i>)		
PHP-232	GGTGGCTTCCAGAACAGCGC	<i>cus</i> (B0909_24515)		
PHP-233	TATCGTGCCTGCCACCCTG	<i>cus</i> (B0909_24515)		
PHP-234	TACCATAGAGGTTGCTCGGCTG	B0909_24450		
PHP-235	GATTCACCGCTGACAACGGC	B0909_24450		
PHP-087	GCGGGCTAAGGTCAAGAAGA	<i>rolB</i> (B0909_24535)		
PHP-088	AAAATGCTAGCCACTACTATGAC	<i>rolB</i> (B0909_24535)		
PHP-089	GCCCATCAATCGTTTTAGAGCC	<i>rolC</i> (B0909_24530)		
PHP-090	TGCATGGGAAGCAGAGGTAT	<i>rolC</i> (B0909_24530)		
PHP-252	GCAAAC T CGTTCTCCTTGAAAAAC	<i>orf13</i> (B0909_24525)		
PHP-253	CCAGTTGTCTGCTATAAATCTTGC	<i>orf13</i> (B0909_24525)		
Curing				
CROPGEN577	CCTGGGCTCTGGTGATTCAG	UGI Fw		
CROPGEN578	TCACTAAATAATAGTGAACGGCAGG	<i>sacB</i> Rv		

Multiplexing

CROPGEN585	ATATATGGTCTCTTAGCTCCCAGATCGAACGGTCGTTGTT	<i>recA (Atu1874)</i>
CROPGEN586	CTCCCAGATCGAACGGTCGTTGTTTTAGAGCTAGAAATAGC	<i>recA (Atu1874)</i>
CROPGEN587	AACGGCTCATCAGACGGGCCTGAAGGCTAGCATTATACCTAGGAC	<i>recA (Atu1874)</i>
CROPGEN588	ATTATTGGTCTCTAAACGGCTCATCAGACGGGCCTGAAGGCT	<i>recA (Atu1874)</i>

Table S3. Spacers used

Gene	Organism	Strain	Spacer (5'-3')
<i>Atu1060</i>	<i>A. tumefaciens</i>	EHA101	GCAGGCCAATAATTTTCACGC
		EHA105	
<i>Atu4309</i>	<i>A. tumefaciens</i>	EHA101	ACCATTTCACACAGGATCGGC
		EHA105	
<i>recA (Atu1874)</i>	<i>A. tumefaciens</i>	EHA105	TCCCAGATCGAACGGTCGTT
<i>recA (Atu1874)</i>	<i>A. tumefaciens</i>	EHA105	CTTCAGGCCCGTCTGATGAGCC
<i>cus (B0909_24515) and B0909_24450</i>	<i>A. rhizogenes</i>	K599	GACCAGTCGATGTACACG
<i>rolB (B0909_24535)</i>	<i>A. rhizogenes</i>	K599	CACGAGATCTCACAAAAGCC
<i>rolB (B0909_24535)</i>	<i>A. rhizogenes</i>	K599	GCCAAGCAATGTTGTGAGCA
<i>rolC (B0909_24530)</i>	<i>A. rhizogenes</i>	K599	TCCAGAGCGCCTCAAAGGAG
<i>orf13 (B0909_24525)</i>	<i>A. rhizogenes</i>	K599	CTCAGCTTGTTAATGTGG

Legends Datasets

Dataset S1. Base editing efficiency. The table lists for each colony the strain, the targeted gene, and the protospacer together with the percentage total peak area of the Sanger sequencing reads corresponding to an edit significantly different from noise at the various protospacer positions. Data for the targeted C are in bold. *sacB* indicates whether *sacB* was present in the construct.

Dataset S2. SNP comparison of the EHA105 hybrid assembly to the *Agrobacterium tumefaciens* C58 reference genome (NC_003062, NC_003063, and NC_003064) and pTiBo542 (DQ058764). The table presents the location of the mutation in the NCBI database, equivalent genomic locus tags for the genomic region in the hybrid assembly (GCA_903772965), the nucleotide and amino acid positions of SNV when encoded on an annotated gene, the gene name and its protein function determined by Prokka, the mutation type, the mutation effect, the reference nucleotide, and the alternate allele at the position. SNV, single-nucleotide variant; INS, insertion; DEL, deletion; FS, frameshift.

Dataset S3. SNV comparisons between the base-edited *Agrobacterium* spp. strains and the sequenced reference parent strains. The table presents the strain, the SNV location in the hybrid assembly (GCA_903772965 and GCA_903772885), the equivalent NCBI genomic locus tags for the genomic region, the nucleotide and amino acid positions of SNV when encoded on an annotated gene, the gene name and its protein function determined by Prokka, the sequence information for five nucleotides upstream and 30 nucleotides downstream of the SNV, the mutation type, the mutation effect, the reference nucleotide, and the alternate allele at the position. SNV, single-nucleotide variant; INS, insertion; DEL, deletion.; FS, frameshift.

SI REFERENCES

1. E. E. Hood, G. L. Helmer, R. T. Fraley, M.-D. Chilton, The hypervirulence of *Agrobacterium tumefaciens* A281 is encoded in a region of pTiBo542 outside of T-DNA. *J. Bacteriol.* **168**, 1291–1301 (1986).
2. E. E. Hood, S. B. Gelvin, L. S. Melchers, A. Hoekema, New *Agrobacterium* helper plasmids for gene transfer to plants. *Transgenic Res.* **2**, 208–218 (1993).
3. J. Tempé, A. Petit, M. Holsters, M. Van Montagu, J. Schell, Thermosensitive step associated with transfer of the Ti-plasmid during conjugation: Possible relation to transformation in crown gall. *Proc. Natl. Acad. Sci. USA* **74**, 2848-2849 (1977).
4. E. R. Morton, C. Fuqua, Genetic manipulation of *Agrobacterium*. *Curr. Protoc. Microbiol.* **25**, 3D.2.1-3.D.2.15 (2012).
5. P. Hajdukiewicz, Z. Svab, P. Maliga, The small, versatile pPZP family of *Agrobacterium* binary vectors for plant transformation. *Plant Mol. Biol.* **25**, 989–994 (1994).
6. A. Lampropoulos *et al.*, GreenGate - A novel, versatile, and efficient cloning system for plant transgenesis. *PLoS ONE* **8**, e83043 (2013).
7. D. Sengupta, D. Chakravarti, U. Maitra, Relative efficiency of utilization of promoter and termination sites by bacteriophage T3 RNA polymerase. *J. Biol. Chem.* **264**, 14246–14255 (1989).
8. T. Aparicio, V. de Lorenzo, E. Martínez-García, CRISPR/Cas9-based counterselection boosts recombineering efficiency in *Pseudomonas putida*. *Biotechnol. J.* **13**, e1700161 (2018).
9. A. Houbaert *et al.*, POLAR-guided signalling complex assembly and localization drive asymmetric cell division. *Nature* **563**, 574–578 (2018).
10. M. E. Lee, W. C. DeLoache, B. Cervantes, J. E. Dueber, A highly characterized yeast toolkit for modular, multipart assembly. *ACS Synth. Biol.* **4**, 975–986 (2015).
11. M. Karimi, A. Depicker, P. Hilson, Recombinational cloning with plant Gateway vectors. *Plant Physiol.* **145**, 1144–1154 (2007).
12. S. Banno, K. Nishida, T. Arazoe, H. Mitsunobu, A. Kondo, Deaminase-mediated multiplex genome editing in *Escherichia coli*. *Nat. Microbiol.* **3**, 423–429 (2018).
13. W. Decaestecker *et al.*, CRISPR-TSKO: A technique for efficient mutagenesis in specific cell types, tissues, or organs in Arabidopsis. *Plant Cell* **31**, 2868–2887 (2019).
14. Z. Hu *et al.*, Genome editing-based engineering of *CESA3* dual cellulose-inhibitor-resistant plants. *Plant Physiol.* **180**, 827–836 (2019).
15. H.-L. Xing *et al.*, A CRISPR/Cas9 toolkit for multiplex genome editing in plants. *BMC Plant Biol.* **14**, 327 (2014).
16. C. Kuscu *et al.*, CRISPR-STOP: Gene silencing through base-editing-induced nonsense mutations. *Nat. Methods* **14**, 710–712 (2017).
17. M. G. Kluesner *et al.*, EditR: A method to quantify base editing from Sanger sequencing. *CRISPR J.* **1**, 239–250 (2018).
18. A. A. Wise, Z. Liu, A. N. Binns, Culture and maintenance of *Agrobacterium* strains. *Methods Mol. Biol.* **343**, 3–13 (2006).
19. A. A. Wise, A. N. Binns, The receiver of the *Agrobacterium tumefaciens* VirA histidine kinase forms a stable interaction with VirG to activate virulence gene expression. *Front. Microbiol.* **6** (2016).

20. V. Jonckheere, D. Fijałkowska, P. Van Damme, Omics assisted N-terminal proteoform and protein expression profiling on methionine aminopeptidase 1 (MetAP1) deletion. *Mol. Cell. Proteomics* **17**, 694-708 (2018).
21. M. Karimi, D. Inzé, M. Van Lijsebettens, P. Hilson, Gateway vectors for transformation of cereals. *Trends Plant Sci.* **18**, 1-4 (2013).
22. G. Coussens *et al.*, *Brachypodium distachyon* promoters as efficient building blocks for transgenic research in maize. *J. Exp. Bot.* **63**, 4263-4273 (2012).
23. R. A. Jefferson, T. A. Kavanagh, M. W. Bevan, GUS fusions: β -glucuronidase as a sensitive and versatile gene fusion marker in higher plants. *EMBO J.* **6**, 3901-3907 (1987).
24. M. D. Abràmoff, P. J. Magalhães, S. J. Ram, Image processing with imageJ. *Biophotonics Int.* **11**, 36-41 (2004).
25. S. Desmet *et al.*, Differential efficiency of wild type rhizogenic strains for *rol* gene transformation of plants. *Appl. Microbiol. Biotechnol.* **103**, 6657-6672 (2019).
26. R. R. Wick, L. M. Judd, K. E. Holt, Performance of neural network basecalling tools for Oxford Nanopore sequencing. *Genome Biol.* **20**, 129 (2019).
27. A. M. Bolger, M. Lohse, B. Usadel, Trimmomatic: a flexible trimmer for Illumina sequence data. *Bioinformatics* **30**, 2114-2120 (2014).
28. R. R. Wick, L. M. Judd, C. L. Gorrie, K. E. Holt, Completing bacterial genome assemblies with multiplex MinION sequencing. *Microb. Genom.* **3**, e000132 (2017).
29. R. R. Wick, L. M. Judd, C. L. Gorrie, K. E. Holt, Unicycler: Resolving bacterial genome assemblies from short and long sequencing reads. *PLOS Comput. Biol.* **13**, e1005595 (2017).
30. R. R. Wick, M. B. Schultz, J. Zobel, K. E. Holt, Bandage: interactive visualization of *de novo* genome assemblies. *Bioinformatics* **31**, 3350-3352 (2015).
31. E. Afgan *et al.*, The Galaxy platform for accessible, reproducible and collaborative biomedical analyses: 2018 update. *Nucleic Acids Res.* **46**, W537-W544 (2018).
32. T. Seemann, Prokka: rapid prokaryotic genome annotation. *Bioinformatics* **30**, 2068-2069 (2014).
33. A. R. Wattam *et al.*, Improvements to PATRIC, the all-bacterial Bioinformatics Database and Analysis Resource Center. *Nucleic Acids Res.* **45**, D535-D542 (2017).
34. A. J. Page *et al.*, Roary: rapid large-scale prokaryote pan genome analysis. *Bioinformatics* **31**, 3691-3693 (2015).
35. M. J. Sullivan, N. K. Petty, S. A. Beatson, Easyfig: A genome comparison visualizer. *Bioinformatics* **27**, 1009-1010 (2011).
36. R. Poplin *et al.*, Scaling accurate genetic variant discovery to tens of thousands of samples. bioRxiv: 10.1101/201178 (24 July 2018).
37. E. Garrison, G. Marth, Haplotype-based variant detection for short-read sequencing. arxiv: 1207.3907v2 [q-bio.GN] (20 July 2012).
38. H. Li, R. Durbin, Fast and accurate short read alignment with Burrows-Wheeler transform. *Bioinformatics* **25**, 1754-1760 (2009).
39. P. Cingolani *et al.*, Using *Drosophila melanogaster* as a model for genotoxic chemical mutational studies with a new program, SnpSift. *Front. Genet.* **3**, 35 (2012).
40. P. Danecek *et al.*, The variant call format and VCFtools. *Bioinformatics* **27**, 2156-2158 (2011).
41. A. McKenna *et al.*, The Genome Analysis Toolkit: a MapReduce framework for analyzing next-generation DNA sequencing data. *Genome Res.* **20**, 1297-1303 (2010).

42. P. Cingolani *et al.*, A program for annotating and predicting the effects of single nucleotide polymorphisms, SnpEff: SNPs in the genome of *Drosophila melanogaster* strain w¹¹¹⁸; *iso-2*; *iso-3*. *Fly* **6**, 80-92 (2012).
 43. H. Thorvaldsdóttir, J. T. Robinson, J. P. Mesirov, Integrative Genomics Viewer (IGV): high-performance genomics data visualization and exploration. *Brief. Bioinform.* **14**, 178-192 (2013).
-